STAGE REPORT

active vibration control by combined feedforward and feedback compensation

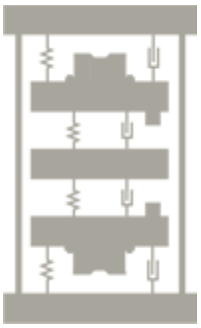

Vuong V. Trinh

Feb – June 2014, GIPSA-lab

Responsables:
Luc Dugard
Ioan D. Landau

Jury:
Gildas Besancon
Mirko Fiacchini

13 June 2014, Grenoble, FRANCE

"This work has been partially supported by the LabEx PERSYVAL-Lab (ANR-11-LABX-0025-01)"

Abstract:

In this stage, solutions for the design of optimal feedforward & feedback compensators for active vibration control systems are presented. The control design takes advantages of perfect knowledge about plant and disturbances characteristics. The techniques of parametric identification, robust control design and controller reduction were employed. The results show that it is possible to simultaneously attenuate broadband and narrowband disturbances.

The report is organized as follows. Section 1 introduces the general problem, the general techniques and the stage motivation as well. Section 2 is dedicated to the presentation of the active vibration control system using an inertial actuator and the parametric identification result. Section 3, presents the design and tuning of H_∞ central controller in order to compensate broadband disturbances. The attenuation of broadband and narrowband disturbances is presented in section 4 and section 5 by means of Youla–Kučera parametrization. Concluding remarks and future works are summarized in section 6. Some details concerning the system identification in open loop operation are given in Appendix A. Some details concerning order reduction of central controller by means of closed loop identification is discussed in Appendix B. The attenuation of broadband and narrowband disturbances by re-computing feedforward and feedback controllers is presented in Appendix C.

The experiment is carried out on the flexible mechanical structure of active vibration control located at the Control Systems Department of GIPSA-Lab, Grenoble, France.

Keywords: parametric identification, H_∞ control, controller reduction, Youla–Kučera parametrization, active vibration control

Contents

1. Introduction

In many classes of applications such as active vibration control and active noise control, the disturbance acting upon a system and which have to be compensated can be characterized by their frequencies content and their location in a specific region in the frequency domain. The disturbances can be of narrowband type or of broadband type. Of course a combination of both is possible and what we call broadband may be in certain cases finite band disturbances over a small region in the frequency domain. However, distinction between these two types of disturbances is convenient in order to examine the techniques used for their compensation.

Previous research was focused on adaptive rejection of unknown narrowband disturbances using a feedback approach or adaptive feedforward compensation of broadband disturbances. Several configurations has been developed, analyzed and evaluated as follow:

- Adaptive feedforward compensation (with/without a fixed feedback controller) of broadband disturbances
- Adaptive feedback regulation of narrowband disturbances

In one hand, feedforward compensation requires the use of well-located transducer to obtain a correlated measurement of disturbances and need to deal with instability risk related to positive coupling. In another hand, feedback compensation can attenuate narrowband disturbances without feedforward compensation. However, broadband disturbances attenuation will require to use feedforward compensation since feedback controller is limited by Bode Integral of the output sensitivity function. For more information, see [6].

Hence, the combined feeddforward and feedback compensation of broadband and narrowband disturbances should be considered. The work of this stage prepares for the development of appropriate adaptive control methodologies for such objective. One can consider.

A very important hypothesis is that the plant model's parameters do not change over time. The design of optimal fixed feedforward and feedback compensators here takes advantages of perfect knowledge about plant model and disturbance characteristics. The design in linear context with perfect knowledge is necessary in order to assess the possible benefits of combined feedforward and feedback compensation. Nevertheless, adaptive algorithms have still not been developed in this stage.

The most significant contribution of this stage is that it reveals the possibility of simultaneous attenuation of broadband and narrowband disturbances using combined feedforward and feedback control.

2. An active vibration control system using an inertial actuator

This section describes the AVC (active vibration control) system and basic notions (Sub-section 2.1). Also, the identification results are presented (Sub-section 2.2). Some remarks in robust control design and control specifications are given (Sub-section 2.3).

2.1. System description and notions

Figs. 1 and 2 show an AVC system applied to a distributed flexible mechanical structure. The corresponding block diagram is shown in Fig. 3. This is representative for a number of situations encountered in practice and will be used to illustrate the performance of various controllers designed in this report.

Figure 1. The flexible mechanical structure for active vibration control system

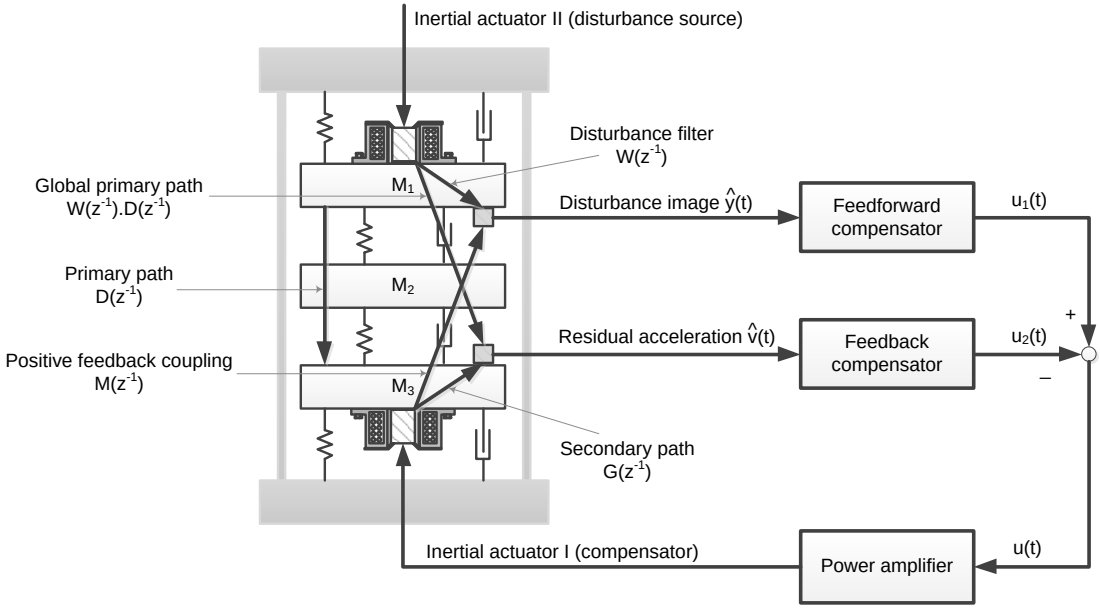

Figure 2. The AVC system using feedforward & feedback compensation

This mechanical structure consists of five metal plates connected by springs. The uppermost and lowermost ones are rigidly jointed together by four screws. The middle three plates will be

labeled for easier referencing M1, M2 and M3. M1 and M3 are equipped with inertial actuators. The one on M1 serves as disturbances generator (inertial actuator I), the one at the bottom serves for disturbances compensation (inertial actuator II). The correlated measurement with the disturbance (image of the disturbance) $\hat{y}(t)$ is obtained from an accelerometer which is positioned on plate M1. Another sensor of the same type is positioned on plate M3 and serves for measuring the residual acceleration. The objective is to minimize the residual acceleration $\hat{v}(t)$ measured on plate M3.

When the compensator system is active, the actuator acts upon the residual acceleration, but also upon the measurement of the image of the disturbance through the reverse path (positive feedback coupling). The disturbance is the position of the mobile part of the inertial actuator located on top of the structure. The input to the compensator system is the position of the mobile part of the inertial actuator located on the bottom of the structure. In addition, the disturbance image and residual acceleration are measured by accelerometers. Thus, the global primary path, the secondary path and the reverse path have a double differentiator behavior.

The corresponding block diagram in open loop operation and with the feedforward & feedback compensator system, are shown in Fig. 3(a) and 3(b), respectively.

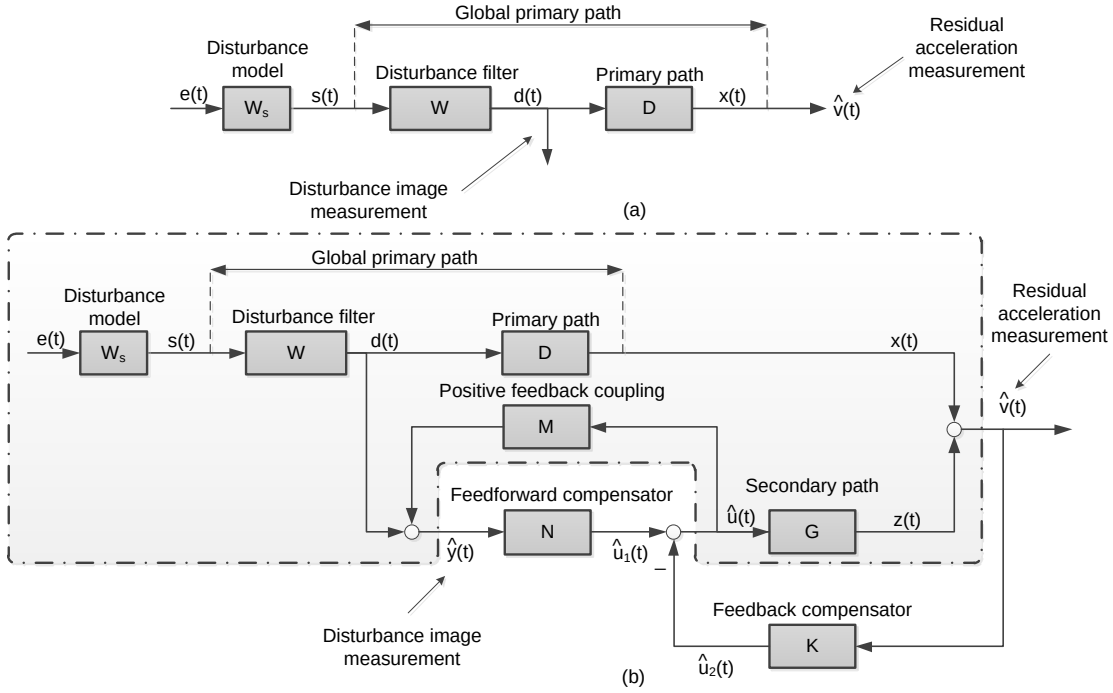

Figure 3. Feedforward & feedback compensation system: (a) in open loop (b) in closed loop

The description of the various blocks will be made with respect to Fig. 3. The complex variable z^{-1} will be used for characterizing the system's behavior in the frequency domain and the delay operator q^{-1} will be used for describing the system's behavior in the time domain.

$$G = \frac{q^{-d_G} B_G}{A_G}, M = \frac{q^{-d_M} B_M}{A_M}, D = \frac{q^{-d_D} B_D}{A_D}, G_p = \frac{q^{-d_{G_p}} B_{G_p}}{A_{G_p}}, W = \frac{q^{-d_W} B_W}{A_W}$$

represent the transfer operators associated with the secondary (G), reverse (M), primary (D) , global primary (G_p) paths and disturbance filter (W) (all asymptotically stable), with

$$B_X(q^{-1}) = b_1^X q^{-1} + \cdots + b_{n_{B_X}}^X q^{-n_{B_X}} = q^{-1} B_X^*(q^{-1})$$

$$A_X(q^{-1}) = 1 + a_1^X q^{-1} + \cdots + a_{n_{A_X}}^X q^{-n_{A_X}} = 1 + q^{-1} A_X^*(q^{-1})$$

for $X \in G, M, D, G_p, W$ and d_X is the pure time delay in number of sampling periods.

The disturbance $s(t)$ can be considered as resulting from the filtering of a white noise $e(t)$ through a shaping filter, i.e.

$$s(t) = W_s(q^{-1}) e(t)$$

Hence, W_s represents the disturbance characteristics.

The optimal feedforward and feedback compensators N and K, computed on the basis of identified paths models and disturbances characteristics, are RS-type digital controllers

$$N(q^{-1}) = \frac{R_N(q^{-1})}{S_N(q^{-1})}, K(q^{-1}) = \frac{R_K(q^{-1})}{S_K(q^{-1})}$$

where the numerator and denominator polynomials are

$$R_X(q^{-1}) = r_0 + r_1^X q^{-1} + \cdots + r_{n_{R_X}}^X q^{-n_{R_X}}$$

$$S_X(q^{-1}) = 1 + s_1^X q^{-1} + \cdots + s_{n_{S_X}}^X q^{-n_{S_X}} = 1 + q^{-1} S_X^*(q^{-1})$$

for $X \in N, K$ and n_{R_X}, n_{S_X} represent the orders of such polynomials.

For different specifications, the polynomials $R_X(q^{-1})$ and $S_X(q^{-1})$ may contain, in general, fixed parts specified. Such specifications are such as zero steady-state error, rejection of sinusoidal disturbance or robustness. In order to take into account these fixed parts, the polynomials $R_X(q^{-1})$ and $S_X(q^{-1})$ are factorized in the form

$$R_X(q^{-1}) = H_{R_X}(q^{-1}) R'_X(q^{-1})$$

$$S_X(q^{-1}) = H_{S_X}(q^{-1}) S'_X(q^{-1})$$

where $H_{R_X}(q^{-1})$ and $H_{S_X}(q^{-1})$ are fixed part polynomials specified, $R'_X(q^{-1})$ and $S'_X(q^{-1})$ are auxiliary part polynomials.

2.2. System identification

Since a model based design approach will be used, identification of the various transfer functions involved is crucial. It is important to remark that in the absence of feedforward & feedback compensators, it is possible to identify the models of required paths. The parametric identification technique used is as in [1]. The details of identification procedure can be found in Appendix A. In this application, a sampling frequency of $800Hz$ has been used.

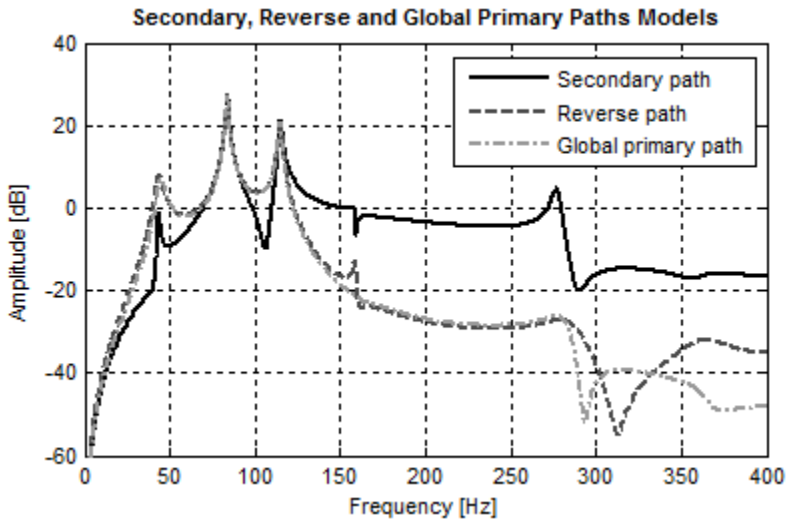

Figure 4. Frequency characteristics of the secondary, reverse and global primary paths models

The secondary path $G(z^{-1})$ between control signal $u(t)$ and the output $v(t)$ has been identified in open-loop operation. The excitation signal was a PRBS of small magnitude generated by a shift register with $N = 9$ and a frequency divider of $p = 2$, applied at the input of the inertial actuator II. The estimated orders of the model are $n_{B_G} = 14, n_{A_G} = 14, d_G = 0$. The best results in terms of model validation were obtained with *Recursive Extended Least Square* method. The frequency characteristic of the secondary path is shown in Fig. 4 (solid line). This model is characterized by three very low damped vibration modes at $43.6Hz$ with a damping of 0.014, at $84Hz$ with a damping of 0.009 and at $115Hz$ with a damping of 0.008. There are two zeros on the unit circle corresponding to the double differentiator behavior and also a pair of low damped complex zeros at $106Hz$ with a damping of 0.017.

The reverse path $M(z^{-1})$ has been identified by the same PRBS excitation applied into $u(t)$ and measuring output signal of the primary transducer $y(t)$. The order of the obtained model is $n_{B_M} = 12, n_{A_M} = 12, d_M = 0$. The best results in terms of model validation were also obtained with *Recursive Extended Least Square* method. The frequency characteristic of the reverse path is presented in Fig. 4 (dashed line). Similarly, there exists several very low damped vibration modes at $43.7Hz$ with a damping of 0.047, at $83.9Hz$ with a damping of 0.008 and at $115Hz$ with a damping of 0.009. There are two zeros on the unit circle corresponding to the double differentiator behavior.

The global primary path $G_p(z^{-1})$ has been also identified using $s(t)$ as an input and measuring $v(t)$. The disturbance $s(t)$ was the same PRBS excitation. The estimated orders of the model are $n_{B_{G_p}} = 14, n_{A_{G_p}} = 14, d_{G_p} = 0$. The frequency characteristic of the reverse path

is presented in Fig. 4 (dashdot line). Similarly, there exists several very low damped vibration modes at $45Hz$ with a damping of 0.045, at $83.9Hz$ with a damping of 0.008 and at $115Hz$ with a damping of 0.008 plus some modes in high frequencies. There are two zeros on the unit circle corresponding to a double differentiator behavior.

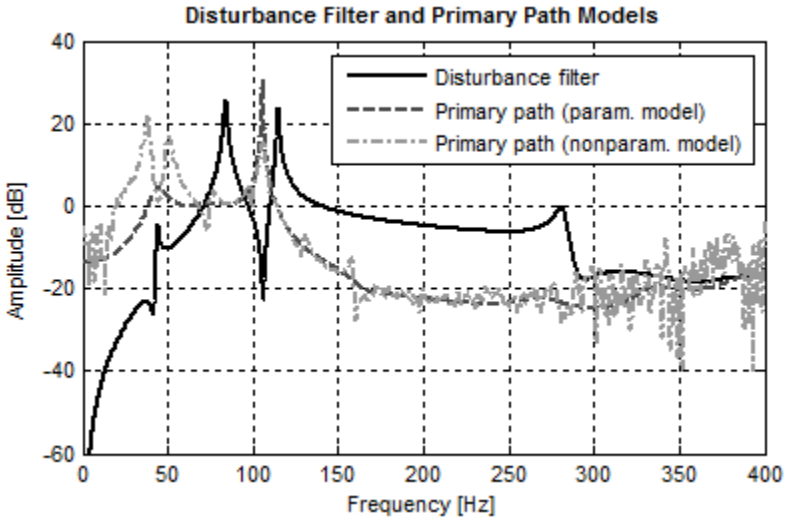

Figure 5. Frequency characteristics of the disturbance filter and primary path models

The model of the disturbance filter $W(z^{-1})$ has been identified by applying excitation into $s(t)$ and measuring output signal of the primary transducer $d(t)$. Due to the symmetry of the mechanical structure, the filter order estimated is the same as for the secondary path $n_{B_W} = 14, n_{A_W} = 14, d_W = 0$. The frequency characteristic of the identified model is presented in Fig. 5 (solid line).

The primary path $D(z^{-1})$ has been identified from the spectrum of the acquired input/output data $d(t)$ and $v(t)$. Since the excitation signal was filtered through disturbance filter $W(z^{-1})$, this model has a good accuracy in the frequency regions where disturbance filter has enough gain. Nevertheless, it has significant error outside such regions. This is illustrated in Fig. 5 where the frequency characteristics of both parametric (dashed line) and nonparametric (dashdot line) models were provided along with that of disturbance filter (solid line). Hence, the primary path model obtained will not be used for control design. Note that the primary path features a strong resonance at $106Hz$, exactly where the secondary path has a pair of low damped complex zeros. Thus, one cannot expect a significant attenuation around this frequency.

At this stage, it is important to remark that the secondary and reverse paths models obtained are very reliable. Thus, it is assumed that these models are equal to the true plants.

2.3. Control specifications

For robustness reason, disturbance compensation can be done only in frequency regions where the secondary path (compensator) has enough gain. If the gain of the controlled system is too low, the disturbance-input sensitivity function will be large at these frequencies. Therefore, the robustness will be reduced and the stress on the actuator will become important. As can be

seen in Fig. 4, the frequency zone of interest is $70Hz \div 150Hz$. Nevertheless, the control will not be able to achieve disturbance cancellation around $106Hz$ where the gain of the secondary path is too low.

It is also important to take into account the fact that the secondary path (the compensator path) has no gain at very low frequencies and very low gain in high frequencies near $0.5f_s$. Thus, the control system has to be designed such that the gains of feedforward & feedback controllers be very low in these regions (preferably 0 at $0.5f_s$). Not taking into account these constraints can lead to undesirable stress of the actuator.

The control objective is to introduce strong attenuation at the narrowband disturbance frequencies, acceptable attenuation of broadband disturbances at the frequency region $70Hz \div 150Hz$ and very little amplification at other frequencies. The operation of the system should remain stable and the control input magnitude should below $0.5V$ in all situations.

Measurements for performance analysis in the frequency domain are:

- Global attenuation (GA) measured in dB and defined by
$$GA = 20 \cdot log \frac{var(v_{cl})}{var(v_{ol})}$$
where v_{ol} and v_{cl} are respectively the residual acceleration in open loop and in closed loop over a certain duration.

- Narrowband disturbance attenuation (DA) measured in dB and defined as the minimum value of the difference between the estimated power spectral density (PSD) of the residual acceleration in closed loop and open loop at narrowband disturbance frequencies:
$$DA = min(PSD_{cl} - PSD_{ol})$$

- Maximum amplification (MA), measured in dB, is defined as the maximum value of the difference between the estimated PSD of the residual acceleration in closed loop and open loop:
$$MA = max(PSD_{cl} - PSD_{ol})$$

The preliminary control specifications are given in Table 1.

Table 1. Control specifications in the frequency domain

Control specifications	**Disturbance = PRBS**	**Disturbance = PRBS + Sinusoids**
Global attenuation	$\leq -17dB$	$\leq -17dB$
Narrowband disturbances attenuation	-	$\leq -30dB$
Maximum output amplification	-	$\leq 9dB$

In addition, the maximum input amplification should below $15dB$.

3. Feedforward & feedback compensation of broadband disturbances

This section presents a procedure for design and tuning of reduced order H_∞ feedforward & feedback compensators for active vibration control system subject to broadband disturbances. Note that the compensators designed in this section will be referred as *central controllers*.

3.1. Central controllers synthesis

The objective is to design two filters $N(q^{-1})$ and $K(q^{-1})$ such that the effect of (finite) broadband disturbance $s(t)$ on the output $v(t)$ be attenuated. In addition, the feedforward filter $N(q^{-1})$ and the feedback filter $K(q^{-1})$ have also to guarantee the stability of the internal positive feedback loop (N-M), the closed loop (G-K) and the coupled feedforward-feedback loop. To do this, the problem has been written as an H_∞ problem by using the appropriate weighting functions as it is shown in Fig. 6(a). In this case, $s(t) = e(t)$ or $W_s(q^{-1}) = 1$.

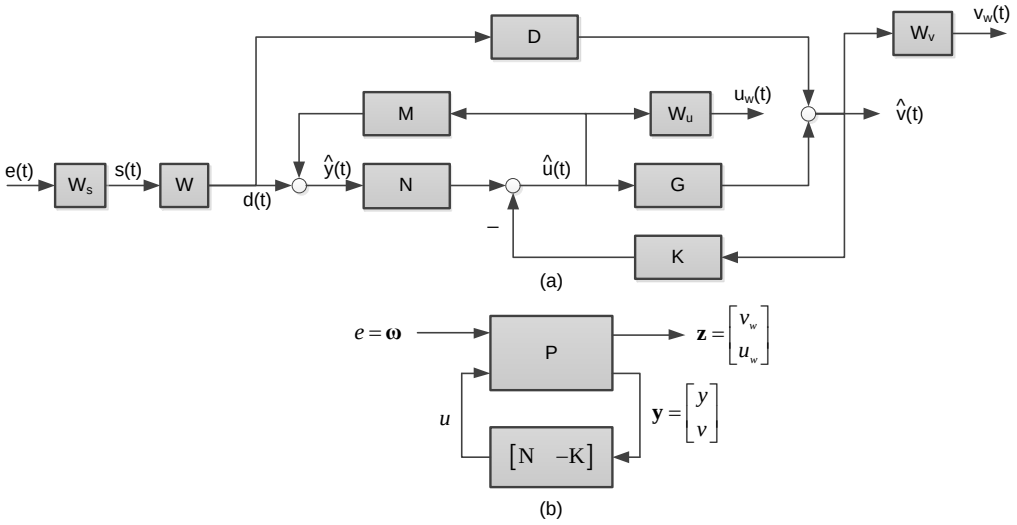

Figure 6. Feedforward & feedback compensation system: (a) design structure (b) generalized plant

The formulation is as in [3]. The weighting functions are used to specify the control objectives. W_u is used to shape the control input to avoid saturation. W_v is used to specify the disturbance frequency regions where the controllers should input energy.

The generalized plant is presented in Fig. 6(b). Using basic algebraic manipulations, it can be shown that the generalized plant is given by

$$\begin{bmatrix} u_w \\ v_w \\ y \\ v \end{bmatrix} = \underbrace{\left[\begin{array}{c|c} 0 & W_s \cdot W_u \\ W_v \cdot W \cdot D & W_s \cdot W_v \cdot G \\ \hline W & W_s \cdot M \\ W \cdot G & W_s \cdot G \end{array}\right]}_{P} \cdot \begin{bmatrix} e \\ u \end{bmatrix}$$

Once the generalized plant has been formulated, feedforward & feedback compensators can be computed via standard H_∞ control design [2].

According to Fig. 6(a), disturbance-output sensitivity function and disturbance-input sensitivity function will be shaped.

$$S_{ve} = W_s W \frac{D + \frac{NG}{1-NM}}{1 + \frac{KG}{1-NM}} \quad S_{ue} = W_s W \frac{1}{1-NM}\left(N - K\frac{D + \frac{NG}{1-NM}}{1 + \frac{KG}{1-NM}}\right)$$

Thus, the H_∞ control problem is to find stabilizing feedforward & feedback compensators $[N \quad -K]$ which minimizes γ such that

$$\left\| \begin{pmatrix} W_v \cdot S_{ve} \\ W_u \cdot S_{ue} \end{pmatrix} \right\|_\infty < \gamma$$

The weighting function W_u was chosen to be constant ($\cong 20$). This choice is motivated by the presence of a low level of the actuator saturations (around $\pm 0.5V$).

The weighting function W_e was chosen to be equal to the reduced order approximation of G, since it is interesting to minimize the residual acceleration $v(t)$ where the secondary path G has enough gain.

The resulting controller has following orders: $n_N = n_{B_N} = n_{A_N} = 70$, $n_K = n_{B_K} = n_{A_K} = 70$.

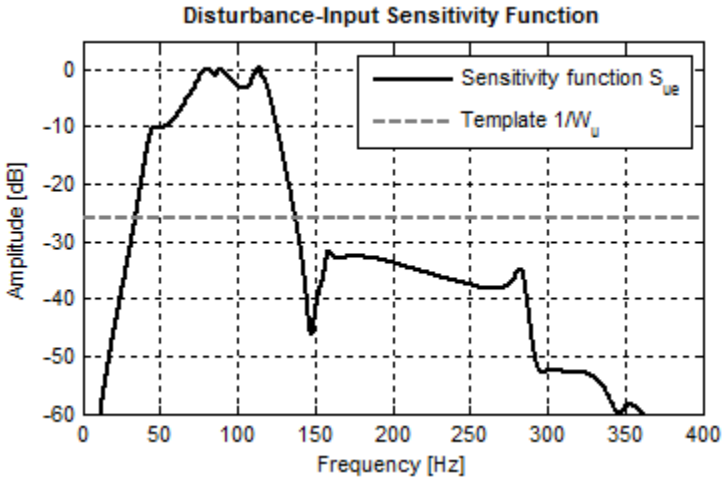

Figure 7. Disturbance-input sensitivity function

As can be seen in Fig. 7, it results that $|S_{ue}|$ is above $|1/W_u|$, however it is very important to see that it is small in the frequency regions where the secondary path has enough gain and less than $0dB$ outside such regions. The compensators open the loop at very low frequencies and high frequencies, guarantee the robustness with respect to unstructured plant model uncertainties (often in high frequencies).

From Fig. 8, one concludes that the compensators give acceptable results for the disturbance rejection over the output $v(t)$ around frequency regions where the secondary path has enough gain. Furthermore, in such regions, the amplification of output sensitivity function is less than $6dB$.

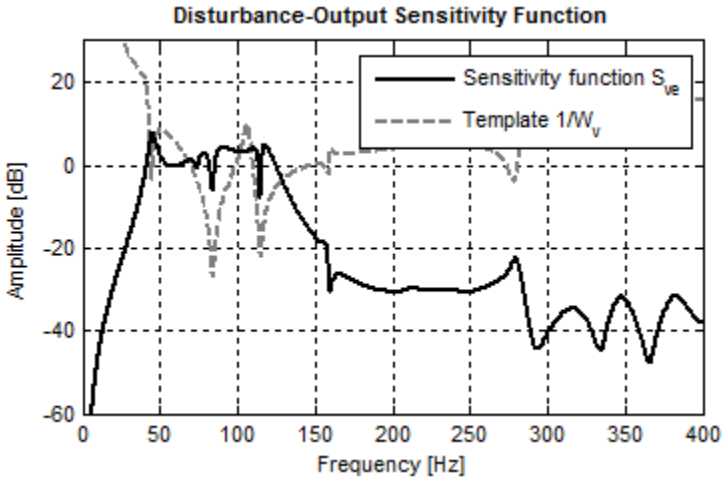

Figure 8. Disturbance-output sensitivity function

3.2. Central controllers order reduction by closed loop identification

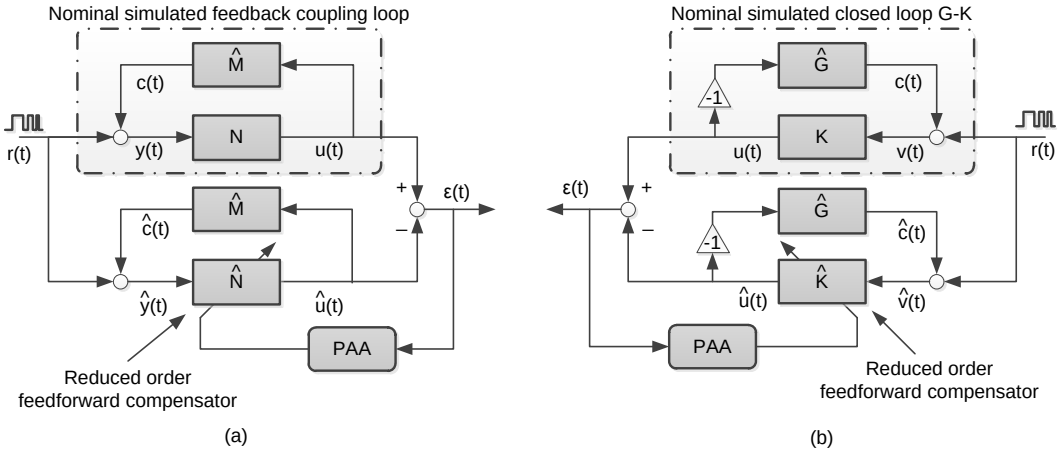

Figure 9. Estimation of reduced order controllers by the method of closed loop input matching (CLIM) with simulated data: (a) feedforward compensator case (b) feedback compensator case

The order reduction of feedforward and feedback controllers will be done separately. The direct identification method for a reduced order controller was employed, with closed loop input matching algorithm (CLIM), based on the simulated data. The methodology and other theoretical details are as in [1] and [4]. As it is shown in Fig. 9, the feedback coupling loop (M-N) and the closed loop (G-K) will be considered, respectively.

The excitation signal was a PRBS generated by a 10-bit shift register, with a clock frequency of $f_s/2$ (data length 4096 samples). A fixed part $H_R = 1 + q^{-1}$ was imposed in the reduced

order controllers in order to open the loop at the frequency $f_s/2$. Good results were obtained with reduced feedforward filter of order $n_{B_{\hat{N}}} = n_{A_{\hat{N}}} = 5, n_{\hat{N}} = 0$ and reduced feedback filter of order $n_{B_{\hat{K}}} = n_{A_{\hat{K}}} = 12, n_{\hat{K}} = 0$. The technical details can be found in Appendix B.

In order to compare the nominal H_∞ feedforward and feedback compensator with the reduced controllers, Fig. 11 shows the frequency characteristics of the obtained compensators using H_∞ control techniques and the reduced ones.

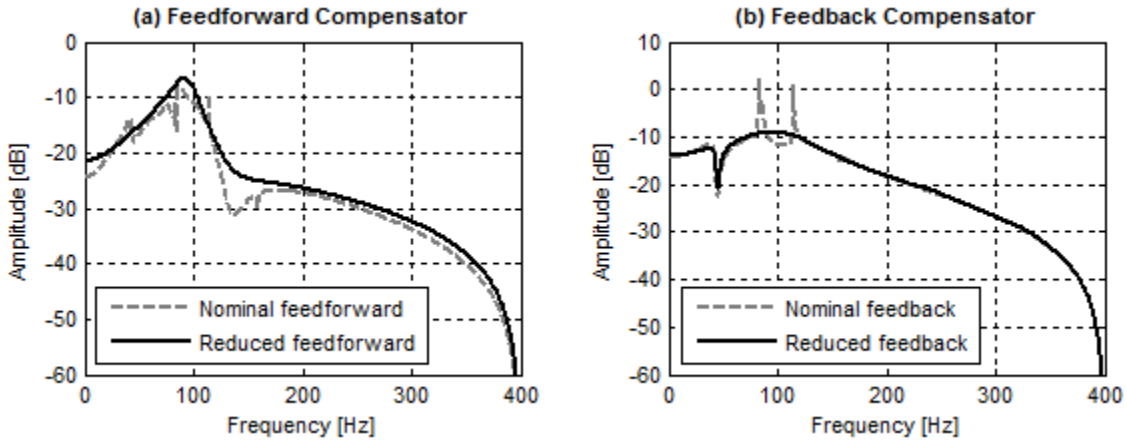

Figure 10. Frequency characteristics of nominal and reduced order controllers
(a) feedforward compensator (b) feedback compensator

3.3. Experimental results

The performance of the system for rejecting broadband disturbances will be illustrated using the feedforward & feedback control scheme with various designed controllers. A PRBS excitation is applied to the inertial actuator as a disturbance (i.e., the mechanical structure is disturbed by an almost white noise filtered by the transfer function of the inertial actuator). The experiments have been carried on by first applying the disturbance in open loop during $50s$ and after that closing the loop with the feedforward & feedback compensation.

Time domain results obtained with and without feedforward & feedback compensators scheme are shown in Figs. 11 and 12. The variance of the residual acceleration in open loop is 0.035. With nominal H_∞ feedforward & feedback compensators, the variance is 0.0046 and it corresponds to a global attenuation of $17.53dB$. With reduced order feedforward & feedback compensators, the variance is 0.0038. This corresponds to a global attenuation of $19.32dB$, which is an improvement with respect to the nominal ones.

Fig. 13 shows the power spectral densities of the residual acceleration obtained in open loop and with feedforward & feedback compensation. One can remarks a strong attenuation in the interested frequency regions. In addition, reduced feedforward & feedback compensators perform slightly better than the nominal compensators.

Table 2 summarizes the results for various configurations.

Table 2. Global attenuation for various configurations

	(1) Adaptive Feedforward only	(2) Feedforward (H_∞) & Feedback (PP)	(3) Adaptive Feedforward & Feedback (PP)	(4) Joint Feedforward & Feedback (H_∞)
Attenuation [dB]	-16.23	-18.42	-20.53	-19.32

In the above table, the configuration (1) adapts the parameters of IIR Q filter with the central feedforward controller designed in [3]. The configuration (2) uses an H_∞ feedforward compensator and a stabilizing feedback controller designed by the standard pole-placement method. The configuration (3) adapts the parameters of IIR Q filter with the central feedforward controller and the same fixed feedback controller as in the configuration (2). Thus, by using H_∞ control design for both feedforward and feedback controllers, the author has improved the result in [3] and approaching the performance of adaptive feedforward and fixed feedback compensators subject to broadband disturbances. Note that one can get better results but the author did not go further. This result, in general, is satisfactory.

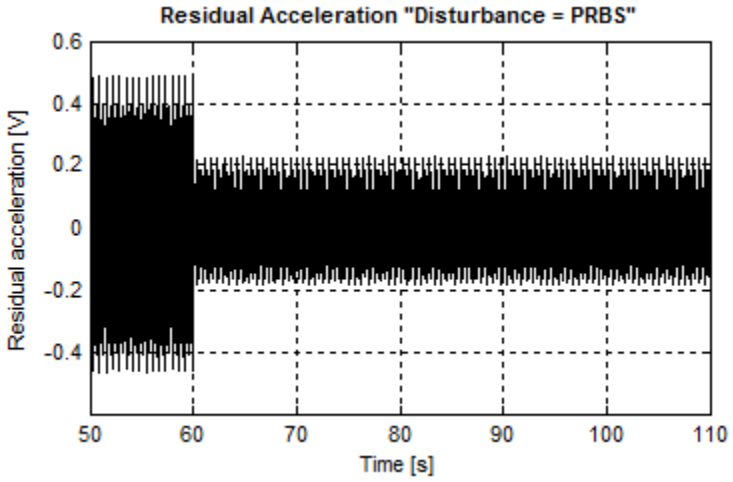

Figure 11. Real time results obtained with nominal H_∞ feedforward & feedback compensators

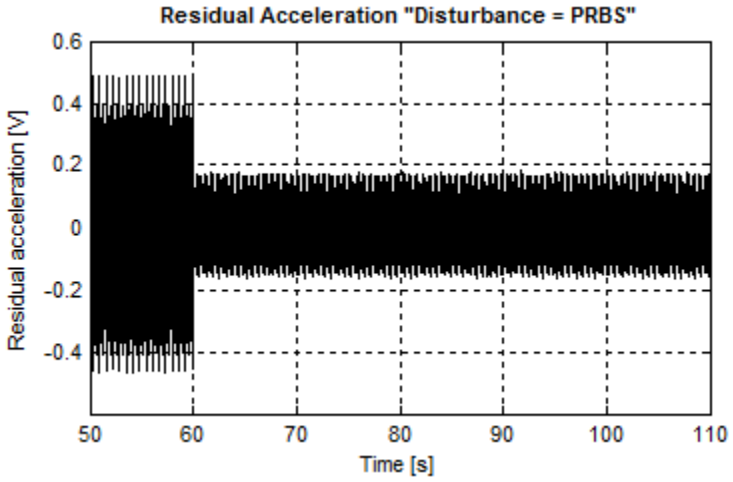

Figure 12. Real time results obtained with reduced H_∞ feedforward & feedback compensators

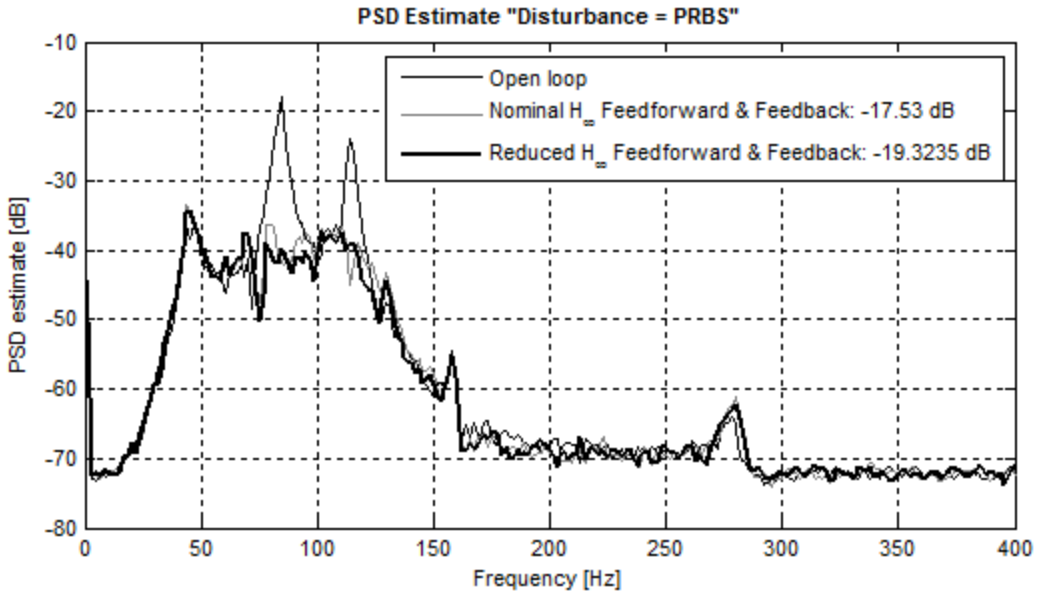

Figure 13. Power spectral densities of the residual acceleration (Disturbance = PRBS)

At this stage, it is important to remark that the performance of central controllers subject to broadband disturbances will be considered as the desired performance. The objective will be to maintain this level of performance under the presence of broadband and narrowband disturbances by tuning central feedforward and feedback controllers.

The re-computing of the central feedforward & feedback controllers is presented in Appendix C. Nevertheless, in the next sections, we only focus on the use of the Youla–Kučera parametrization (or Q-parametrization). IIR (infinite impulse response) Youla–Kučera parametrization will be considered.

In general, under the presence of broadband and narrowband disturbances, there are several approaches for attenuation objective, such as:

- Keep central feedforward controller unchanged, calculate an optimal Q-parameter of feedback controller
- Keep central feedback controller unchanged, calculate an optimal Q-parameter of feedforward controller
- Calculate two optimal Q-parameters of both feedforward and feedback controllers

The first approach is presented in Section 4 while Section 5 is dedicated to the second approach. The third approach should be carried out in the future works.

4. Feedforward & IIR Youla–Kučera parametrized feedback compensation of broadband and narrowband disturbances

The objective in this section is to design the optimal feedback filter $K(R_K, S_K)$ such that the effect of disturbances $s(t)$ (including broadband and single/multi-sinusoidal disturbances) on the output $v(t)$ be attenuated. In addition, the feedback filter K has also to guarantee the stability of the closed loop (G-K). Thus, it turns out that Youla-Kucera parametrization provides good parametrization of the feedback controller.

4.1. Youla–Kučera parametrization of feedback controller

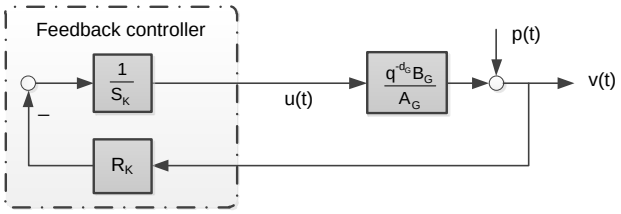

Figure 14. Equivalent system representation

Fig. 14 shows the equivalent system with the control system presented in Fig. 3(b). The RS feedback controller has canonical structure (see [1]). In the analysis of the closed loop (G-K), $u_1(t)$ is considered as control input disturbance. Hence, the control input is considered as $u(t) = -u_2(t)$. The effect of $u_1(t)$ and primary path output are included in the output perturbation $p(t)$ (see Fig. 14).

Let assume that a feedback central controller has been designed such that the closed loop is asymptotically stable and that we are looking to the redesign of the feedback controller in order to reject simultaneously both broadband diturbances and sinusoidal disturbances but without re-computing the central controllers.

Denote the central controllers designed in section 3 as $N_0(R_N^0, S_N^0)$ and $K_0(R_K^0, S_K^0)$. It is assumed that the central feedback controller $K_0(R_K^0, S_K^0)$ stabilizes secondary path model, i.e. the characteristic polynomial of the closed loop (G-K_0)

$$P_{fb}^0 = A_G R_K^0 + q^{-d_G} B_G S_K^0$$

is Hurwitz polynomial.

The feedback compensator stabilizing the secondary path can be written, using IIR Youla-Kucera parametrization, as

$$K(q^{-1}) = \frac{R_K(q^{-1})}{S_K(q^{-1})} = \frac{A_Q(q^{-1}) R_K^0(q^{-1}) + A_G(q^{-1}) B_Q(q^{-1})}{A_Q(q^{-1}) S_K^0(q^{-1}) - q^{-d_G} B_G(q^{-1}) B_Q(q^{-1})}$$

where Q is an asymptotically stable rational proper function

$$Q(q^{-1}) = \frac{B_Q(q^{-1})}{A_Q(q^{-1})} = \frac{b_0^Q + b_1^Q q^{-1} + \cdots + b_{n_{B_Q}}^Q q^{-n_{B_Q}}}{1 + a_1^Q q^{-1} + \cdots + a_{n_{A_Q}}^Q q^{-n_{A_Q}}}$$

Hence, the characteristic polynomial of the closed loop (G-K) is

$$P_{fb} = A_G R_K + q^{-d_G} B_G S_K = A_Q P_{fb}^0$$

Taking into account the hypotheses made upon central feedback controller and $Q(q^{-1})$, it results that the closed loop poles will be asymptotically stable.

The structure of Youla-Kucera parametrized feedback controller is shown in Fig. 15.

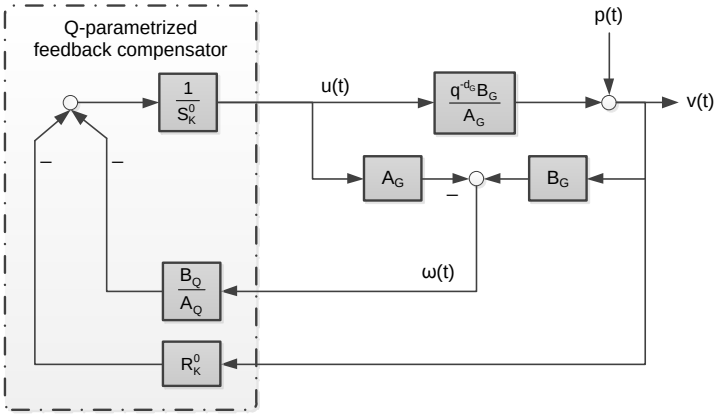

Figure 15. The Youla-Kucera paraemtrized feedback controller

4.2. Feedback Q-parameter synthesis

The objective is to calculate an asymptotically stable filter Q such that the effect of disturbances $s(t)$ (including broadband and a sinusoidal disturbance at $150Hz$) on the output $v(t)$ be minimized. To do this, the problem has been written as an H_∞ problem by using the appropriate weighting functions as it is shown in Fig. 16(a). The generalized plant is presented in Fig. 16(b). The central controllers obtained in Section 3 are used.

In this case, W_s can be considered as a filter with an amplification of $30dB$ at $150Hz$ and the gain of 1 at other frequencies. This consideration motivated from the control specification concerning narrowband disturbances attenuation.

The formulation and synthesizing procedure are similar as in Section 3.

The weighting functions have been chosen as $W_{u}' = W_u$ and $W_{v}' = W_v \cdot H_{BSF}^{-1}$ where W_u and W_v are the corresponding weighting functions used in Section 3.1. H_{BSF} is a bandstop filter (BSF), which will assure the desired attenuation of a narrowband disturbance. This choice motivated from the fact that Q-parameter should input energy at $150Hz$.

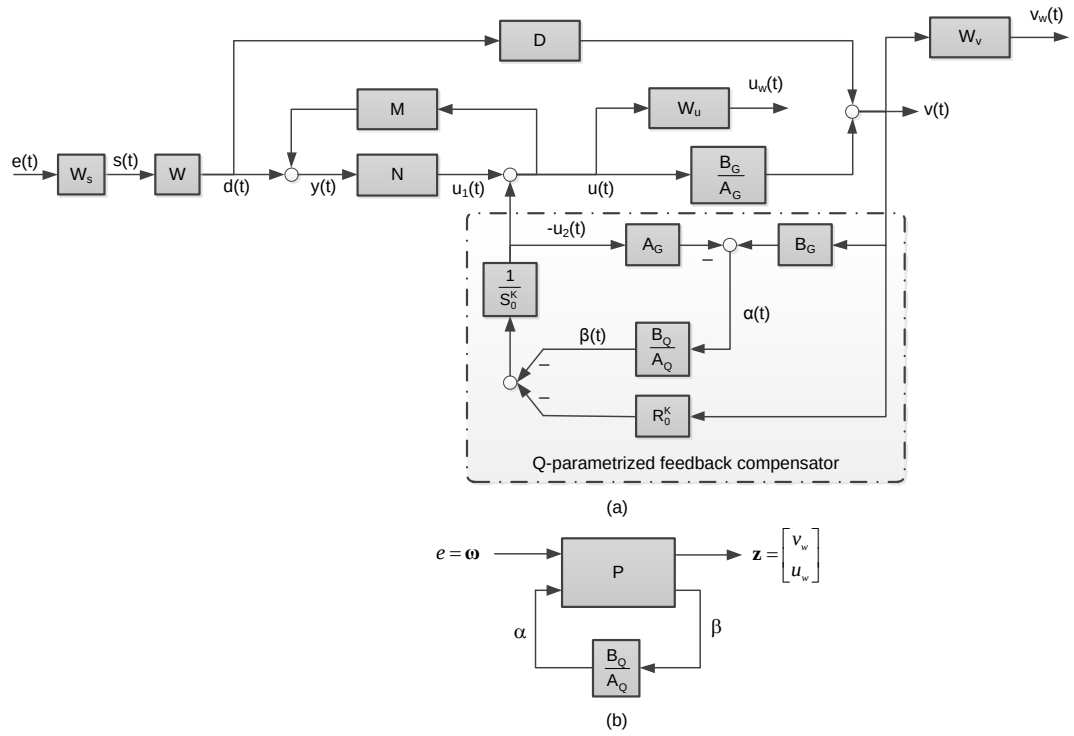

Figure 16. IIRYK parametrized feedback compensation system in the presence of a feedforward controller: (a) design structure (b) generalized plant

The structure of the BSF is

$$H_{BSF}(z^{-1}) = \frac{S_{BSF}(z^{-1})}{P_{BSF}(z^{-1})} = \frac{1+\beta_1 z^{-1}+\beta_2 z^{-2}}{1+\alpha_1 z^{-1}+\alpha_2 z^{-2}}$$

resulting from the discretization of a continuous filter

$$F(s) = \frac{s^2+2\zeta_n \omega s+\omega^2}{s^2+2\zeta_d \omega s+\omega^2}$$

This filter introduces an attenuation of $M = -20\log_{10}\left(\frac{\zeta_n}{\zeta_d}\right)$ at the frequency ω. In this case, $M = -60dB$ and $\omega = 2\pi \cdot 150\ rad/s$ have been chosen.

For n narrowband disturbances, n BSFs will be used

$$H_{BSF}(z^{-1}) = \frac{S_{BSF}(z^{-1})}{P_{BSF}(z^{-1})} = \frac{\prod_{i=1}^{n} S_{BSF_i}(z^{-1})}{\prod_{i=1}^{n} P_{BSF_i}(z^{-1})}$$

The resulting Q-parameter has the orders of $n_Q = n_{B_Q} = n_{A_Q} = 117$. As can be seen from Figs. 17 and 18, one concludes that the obtained Q-parameter gives significant attenuation at $150Hz$ and maintains the level of performance (as in Fig. 13). This is also confirmed by the experimental result (see Fig. 21). $|S_{ue}|$ is typically high at $150Hz$ but still below $15dB$.

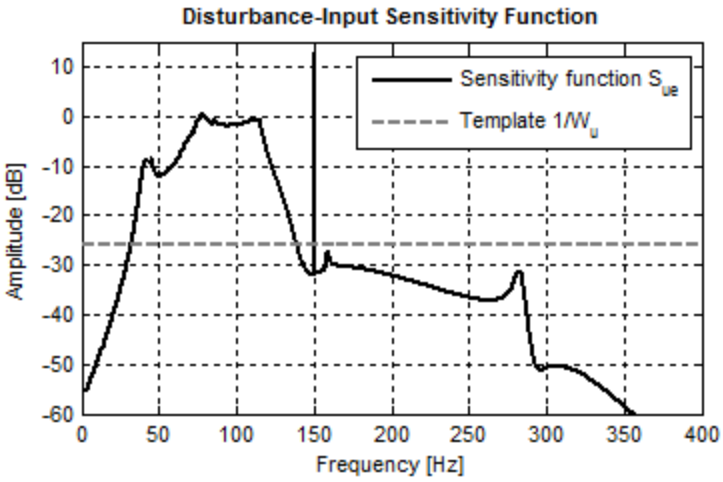

Figure 17. Disturbance-input sensitivity function

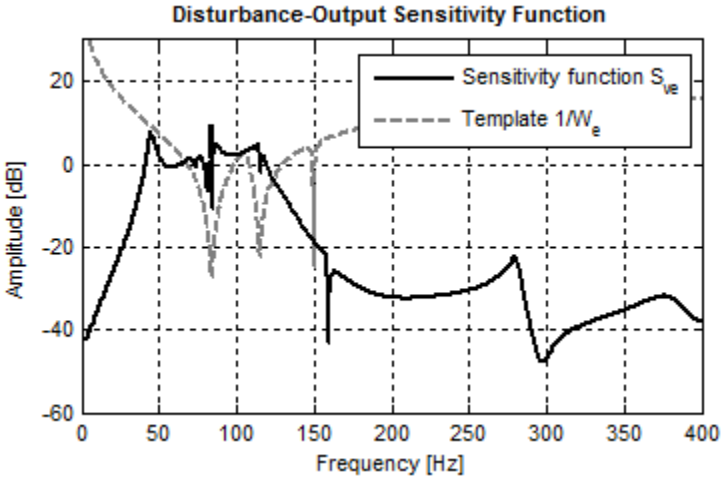

Figure 18. Disturbance-ouput sensitivity function

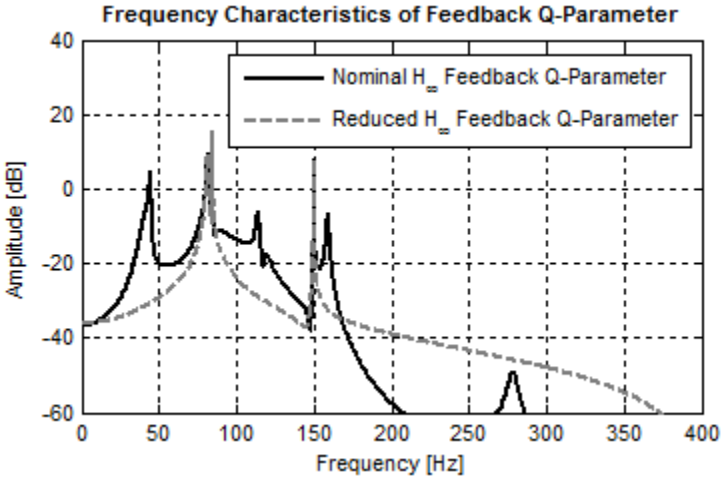

Figure 19. Frequency characteristics of feedback Q parameters

The order reduction of Q without degrading the system performance has been still an open problem and need future works. In this stage, the reduction of Q was carried out by means of standard simplification methods. Good results are obtained with the Q-parameter has the orders of $n_Q = n_{B_Q} = n_{A_Q} = 6$.

As can be seen in Fig. 19, $H_{S_Q}(q^{-1})$ features a pair of undamped complex zeros at $150Hz$. Thus, this result, more or less, is coherent with the standard pole placement design for including the internal model of the disturbance in Q (see [1] and [6]).

4.3. Experimental results

The experimental results are presented in Figs. 20 and 21. One concludes that the level of performance is maintained as in the case of only broadband disturbances are applied. It has been verified that the good performance is still obtained under the presence of additional sinusoidal disturbances.

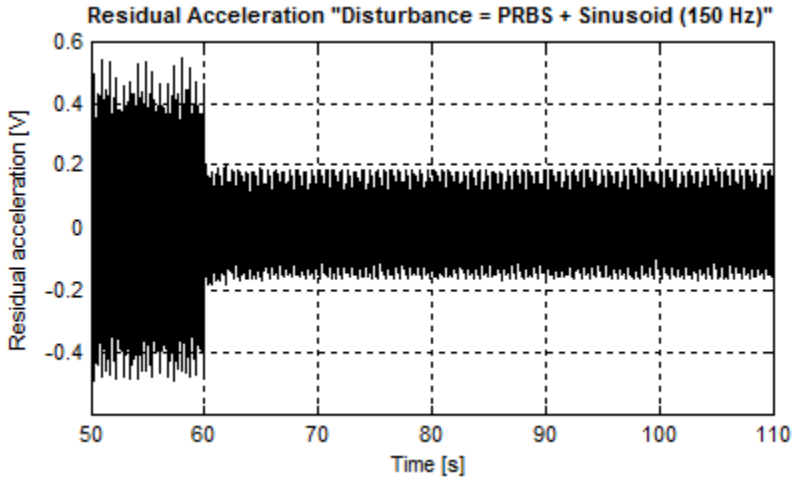

Figure 20. Real time result obtained with feedforward & IIRYK parametrized feedback compensators

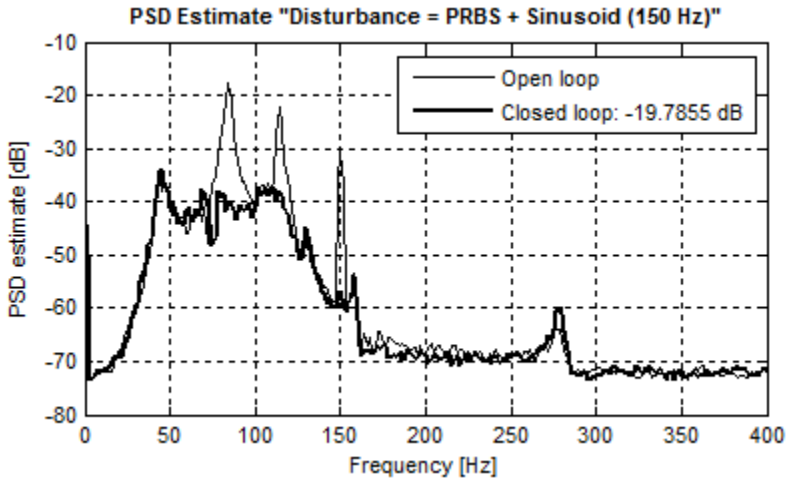

Figure 21. Power spectral densities of the residual acceleration (Disturbance = PRBS + Sinusoid 150Hz)

5. IIR Youla–Kučera parametrized feedforward & feedback compensation of broadband and narrowband disturbansces

The objective in this section is to design the optimal feedforward filter $N(R_N, S_N)$ such that the effect of disturbances $s(t)$ (including broadband and single/multi-sinusoidal disturbances) on the output $v(t)$ be attenuated. In addition, the feedforward filter N has also to guarantee the stability of the closed loop (M-N). Thus, it turns out that Youla-Kucera parametrization provides good parametrization of the feedback controller.

5.1. Youla–Kučera parametrization of feedforward controller

The feedforward compensator stabilizing the reverse path can be written, using IIR Youla-Kucera parametrization, as

$$N(q^{-1}) = \frac{R(q^{-1})}{S(q^{-1})} = \frac{A_Q(q^{-1})R_0(q^{-1}) - B_Q(q^{-1})A_M(q^{-1})}{A_Q(q^{-1})S_0(q^{-1}) - B_Q(q^{-1})B_M(q^{-1})}$$

where Q is an asymptotically stable rational proper function

$$Q(q^{-1}) = \frac{B_Q(q^{-1})}{A_Q(q^{-1})} = \frac{b_0^Q + b_1^Q q^{-1} + \cdots + b_{n_{B_Q}}^Q q^{-n_{B_Q}}}{1 + a_1^Q q^{-1} + \cdots + a_{n_{A_Q}}^Q q^{-n_{A_Q}}}$$

Similarly, the characteristic polynomial of the closed loop (M-N) is

$$P_{ff} = A_M R_N - q^{-d_M} B_M S_N = A_Q(A_M R_N^0 - q^{-d_M} B_M S_N^0) = A_Q P_{ff}^0$$

Taking into account the hypotheses upon stabilizing central feedforward controller and $Q(q^{-1})$, it results that the coupling loop poles will be asymptotically stable.

5.2. Feedforward Q-parameter synthesis

The objective is to calculate an asymptotically stable filter Q such that the effect of disturbances $s(t)$ (including broadband and a sinusoidal disturbance at $150Hz$) on the output $v(t)$ be minimized. To do this, the problem has been written as an H_∞ problem by using the appropriate weighting functions as it is shown in Fig. 22(a). The generalized plant is presented in Fig. 22(b). The central controllers obtained in Section 3 continue to be used.

W_s is as in Section 4 since the same disturbance is considered.

The formulation, synthesizing procedure and the weighting functions selection are similar as in Sub-section 4.1.

The resulting Q-parameter has the orders of $n_Q = n_{B_Q} = n_{A_Q} = 126$. As can be seen from Figs. 23 and 24, one concludes that the obtained Q-parameter gives significant attenuation at $150Hz$ and maintains the level of performance (as in Fig. 13). This is also confirmed by the experimental result (see Fig. 21).

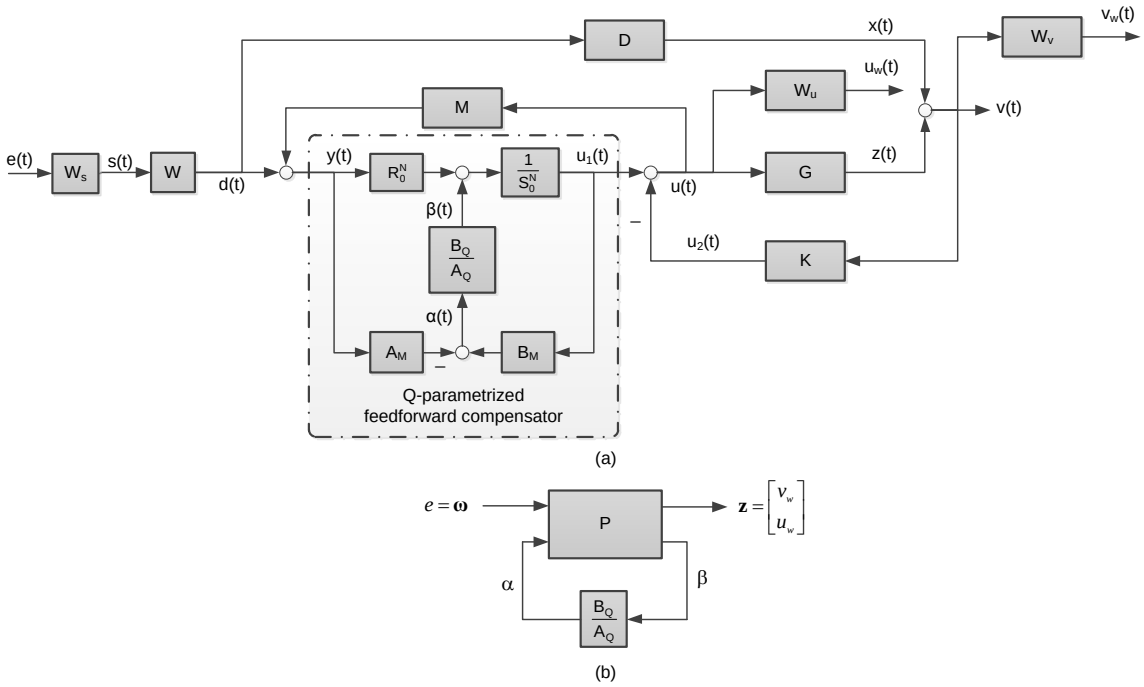

Figure 22. IIRYK parametrized feedforward compensation system in the presence of a feedback controller: (a) design structure (b) generalized plant

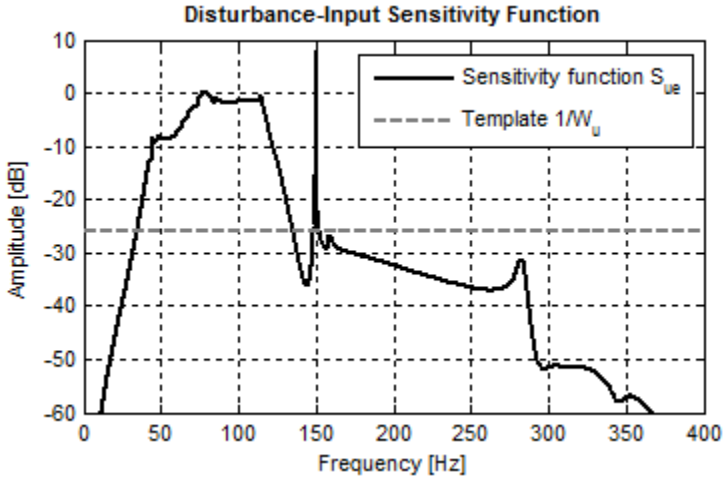

Figure 23. Disturbance-input sensitivity function

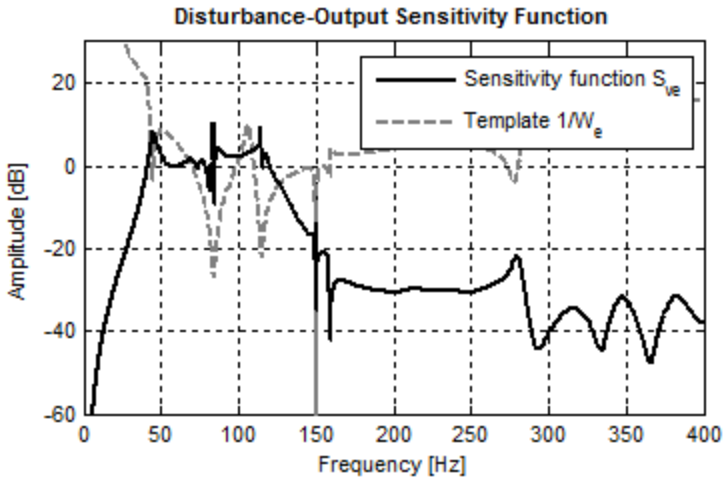

Figure 24. Disturbance-ouput sensitivity function

Good results are also obtained with the reduced-order Q-parameter $n_Q = n_{B_Q} = n_{A_Q} = 20$.

As can be seen in Fig. 25, $H_{S_Q}(q^{-1})$ features a pair of undamped complex zeros at $150Hz$.

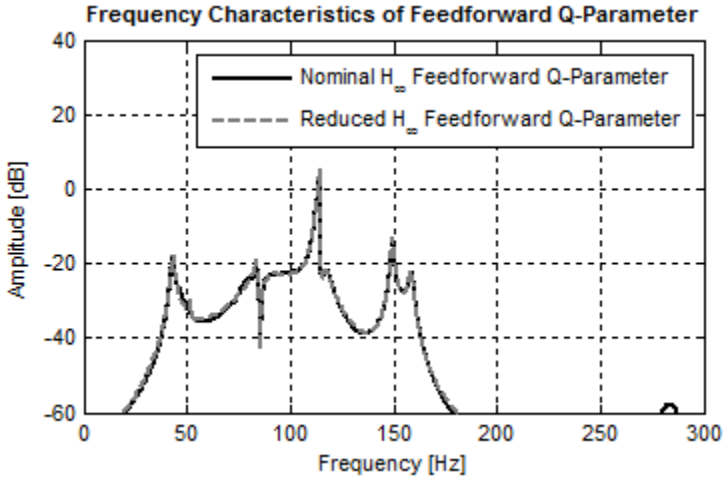

Figure 25. Frequency characteristics of feedforward Q parameters

5.3. Experimental results

The experimental results are presented in Figs. 26 and 27 with reduced-order Q. The performance is similar with the performance of nominal H_∞ Q (not presented here). One concludes that the level of performance is maintained as in the case of only broadband disturbances are applied. One notices that the sinusoidal disturbance attenuation is less effective than the case of tuning the feedback controller. However, this is due to the uncertainties in plant and disturbance model since the simulation gives perfect attenuation at $150Hz$.

It has been also verified that the good performance is still obtained under the presence of additional sinusoidal disturbances.

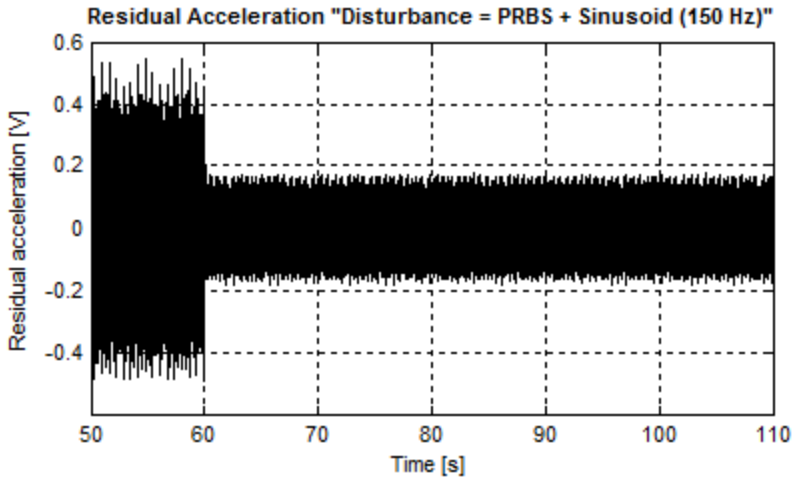

Figure 26. Real time result obtained with IIRYK parametrized feedforward & feedback compensators

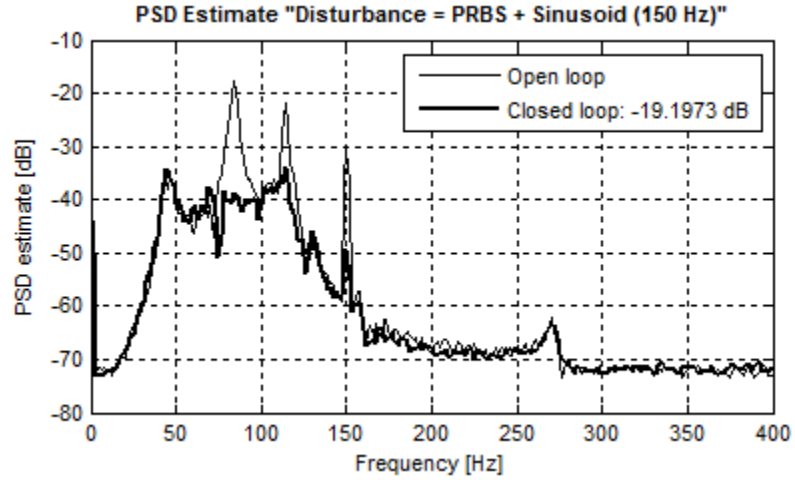

Figure 27. Power spectral densities of the residual acceleration (Disturbance = PRBS + Sinusoid 150Hz)

6. Concluding remarks and future works

The results reveal the possibility of simultaneous compensation of broadband and narrowband disturbances using adaptive feedback + fixed feedforward and adaptive feedforward + fixed feedback. The whole idea is if it is possible to achieve such desired objective in perfect knowledge context, it may also possible in non-perfect knowledge context.

The next step is to develop, analyze and evaluate several adaptive configurations, such as:

- Youla-Kucera parametrized adaptive feedback compensation algorithms in the presence of a feedforward compensators.
- Youla-Kucera parametrized adaptive feedforward compensation algorithms in the presence of a feedback controller.

The expected result is to maintain desired performance level under the effect of broadband and unknown/time-varying narrowband disturbances. An important remark is that attenuation of broadband and two sinusoidal disturbances is a level large enough in most applications.

Another different path of research is to investigate the combination of feedforward and feedback controllers in active vibration control context, hence figure out the possible benefits of adaptive feedforward and adaptive feedback compensation.

Otherwise, the context where the plant model's parameters change in time or a multivariable control approach also have to be considered.

Appendix A
Parametric identification in open loop operation

In this appendix, the identification procedure of the flexible mechanical structure, especially the secondary path, will be examined. A short description of the data acquisition system is shown in Fig. 28. The sampling frequency is $800Hz$ ($T_e = 1.25ms$). The real-time experiments have been performed with different PRBS generated by a shift register with $N = 9,10$ and $p = 2,3,4$ (sequence length 4096 samples, magnitude $0.15V$).

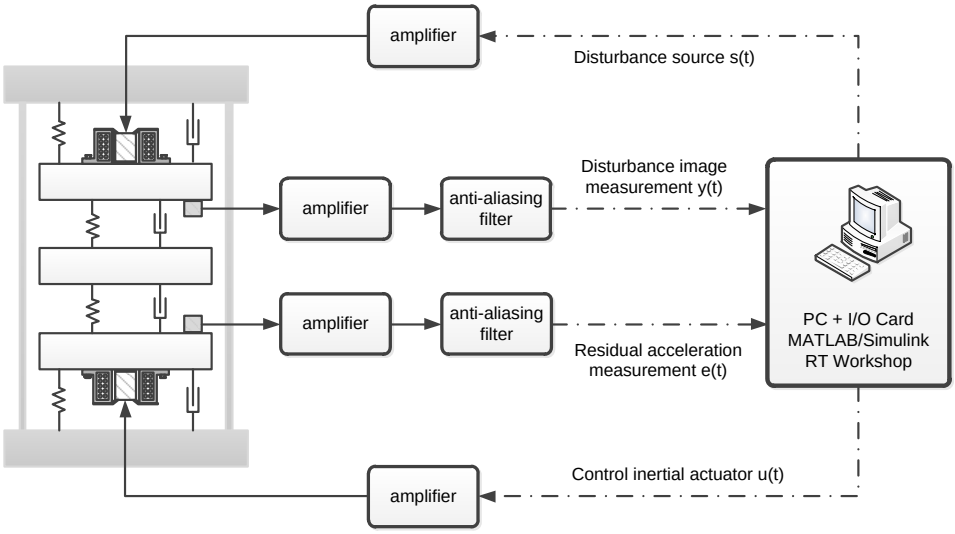

Figure 28. Data acquisition for system identification of the active vibration control platform in open loop operation

The input of secondary path is the voltage applied to a power amplifier that feeds the inertial actuator I, and the output is the residual acceleration measured by means of a tachometer. From the identification point of view, let us consider the cascade power amplifier, inertial actuator, secondary path, tachometer, filter on measured output as the plant.

The DC components (corresponding to the operating point) of I/O data are eliminated. Since the existence of double differentiator behavior is known a priori, one should incorporate it into the model using the filtered data. Specifically, the input is replaced by its double differential, the output remaining the same:

$$u'(t) = (1 - 2q^{-1} + q^{-2})u(t);\ y'(t) = y(t)$$

The estimation of the order for the model has been carried on with several I/O data sets by using the technique of instrumental variables. The order for the secondary path model to be chosen is $n_G = max\left(n_{A_G}, n_{B_G} + d_G\right) = 14$, resulting from the data set $(N = 9, p = 3)$.

One chose "plant+model" structure as ARMAX model. The recursive extended least squares method (RELS) is used and also be compared with the output error with extended prediction model method (XOLOE). The best model in terms of model validation has the order of $n_{A_G} =$

$n_{B_G} = 14$, corresponding to the data set $(N = 9, p = 2)$. The result of identification and validation are given below.

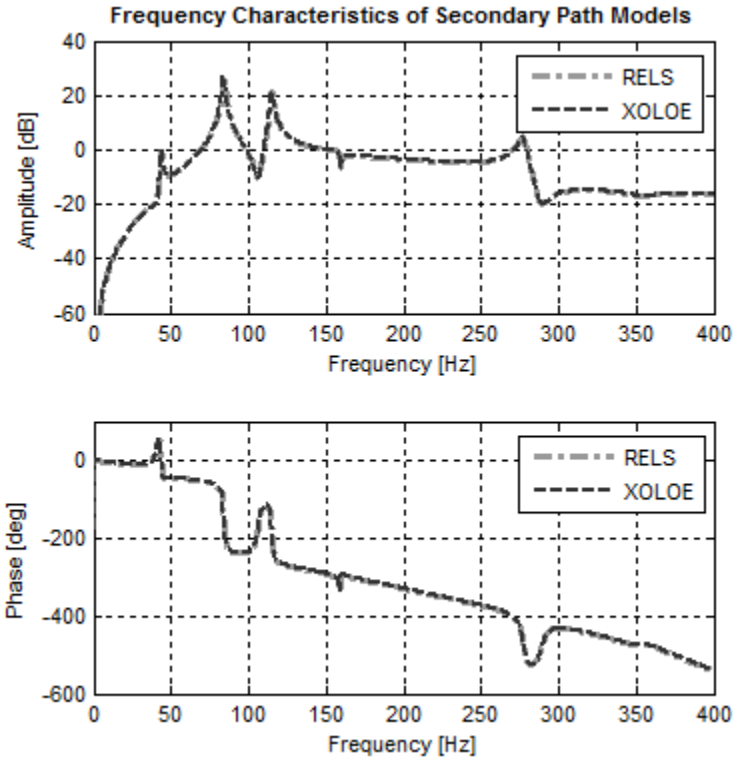

Figure 29. Frequency characteristics of the secondary path models

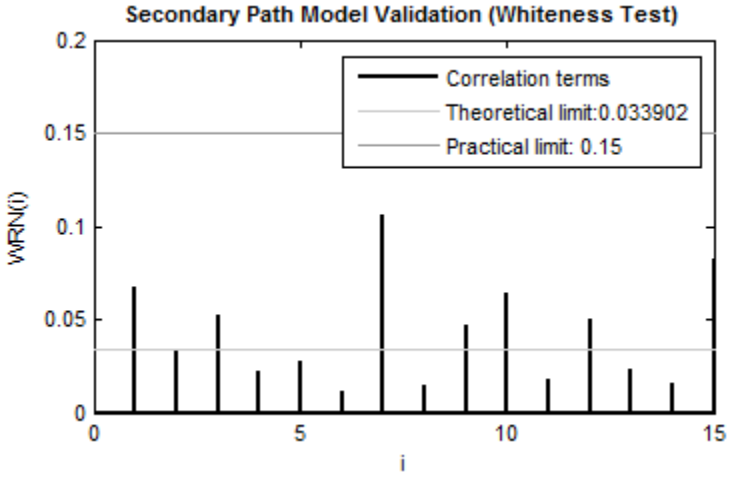

Figure 30. Secondary path model validation

The validation is satisfactory, as all the values $RN(i)$ are smaller than 0.15 for $i = 1,2 \ldots 14$.

The frequency characteristics of this model is shown in Fig. 29 (line RELS). The comparison of the frequency characteristics of the modes identified shows that they are very similar.

As can be seen from the pole-zero map in Fig. 31, there are two zeros on the unit circle, corresponding to the double differentiator behavior. One also notices a pair of pole and zero which are very close.

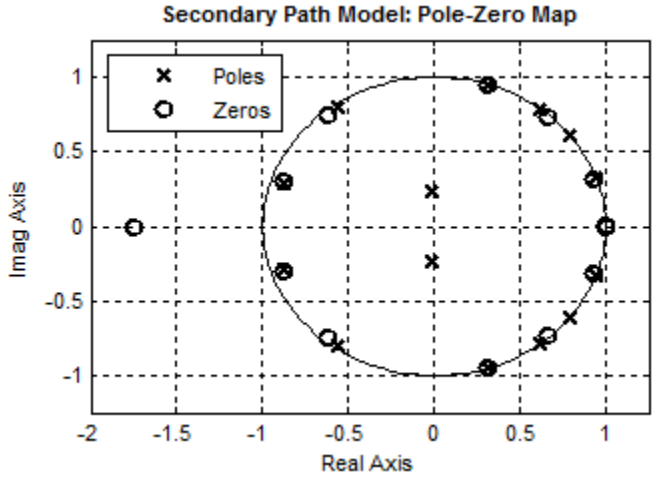

Figure 31. Pole-zero map of the identified model for the secondary path

The identification procedure for the other paths was similar. The results are already presented in Sub-section 2.2.

Appendix B
Central controller order reduction by closed loop identification

In this appendix, the order reduction procedure of the feedforward & feedback compensators will be examined. The complexity of the H_∞ feedforward & feedback filters obtained in Section 3.2 is $n_{R_N} = n_{S_N} = n_{R_K} = n_{S_K} = 70$. We will refer to these controllers as the nominal central controllers (N_n, K_n). Through standard simplification, we obtained (N_1, K_1) characterized by the orders $n_{R_N} = n_{S_N} = n_{R_K} = n_{S_K} = 20$. It has been verified that (N_1, K_1) provides the similar performance in comparison with (N_n, K_n). The order reduction by closed loop identification will be carried out on the basis of (N_1, K_1). Nevertheless, the performance of reduced order controllers will be compared with that of nominal central controllers.

In this specific application, we will look for reduced order controllers with the fixed parts: $H_S = 1, H_R = 1 + q^{-1}$ and stabilize the true plant and the plant model as well.

In Tables 3 and 4, four reduced order feedforward and feedback controllers are considered. Such controllers have been obtained using CLIM algorithm and simulated data. The values found for the Vinnicombe normalized distance (δ_v, row 1 and row 2) (see [1]) give a first indication of the proximity between the sensitivity functions computed with N_1 (or K_1) and those computed with N_2, N_3, N_4 and N_5 (or K_2, K_3, K_4 and K_5). Row 3 gives the generalized stability margin for each controller.

Table 3. Comparison of the reduced order feedforward controllers in the closed loop (N-M)

Feedforward compensator	N_n $n_R = n_S = 70$	N_1 $n_R = n_S = 20$	N_2 $n_R = n_S = 18$	N_3 $n_R = n_S = 16$	N_4 $n_R = n_S = 12$	N_5 $n_R = n_S = 5$
1 $\delta_v(S_{up}^n, S_{up}^i)$	-	-	1.0000	1.0000	1.0000	1.0000
2 $\delta_v(S_{yp}^n, S_{yp}^i)$	-	-	1.0000	1.3315	1.0000	1.0000
3 $b(N_i, M)$	-	0.0909	0.0910	0.0910	0.0830	0.0829

Table 4. Comparison of the reduced order feedback controllers in the closed loop (G-K)

Feedback compensator	K_n $n_R = n_S = 70$	K_1 $n_R = n_S = 20$	K_2 $n_R = n_S = 16$	K_3 $n_R = n_S = 12$	K_4 $n_R = n_S = 10$	K_5 $n_R = n_S = 6$
1 $\delta_v(S_{up}^n, S_{up}^i)$	-	-	0.0467	1.0000	1.0000	0.2108
2 $\delta_v(S_{yp}^n, S_{yp}^i)$	-	-	1.0000	1.0000	5.0586	3.1148
3 $b(K_i, G)$	-	0.1828	0.2053	0.2070	0.2019	0.1570

Table 5 gives the best performance has been obtained by experimental validation. Clearly controllers (N_5, K_3) and (N_5, K_4) provides very good global attenuations. The very-low order pair of controllers (N_5, K_5) also provides an acceptable performance. Furthermore, they perform significant improvement with respect to the nominal compensators. Thus, we refer (N_5, K_3) as reduced compensators.

Table 5. Comparison of the performance of reduced compensators with that of nominal ones

Compensators	N_n & K_n	N_5 & K_3	N_5 & K_4	N_5 & K_5
Global attenuation	-17.53	-19.32	-19.21	-18.23

In terms of sensitivity functions closeness, from the Tables 3 and 4, reduced compensators provide very good Vinnicombe gap for both S_{up} and S_{yp} (which are equal to S_{ur} and S_{yr},

respectively). This is confirmed by a visual inspection of the sensitivity functions frequency characteristics (see Figs. 32 and 33).

Considering robustness, reduced feedforward controller N_5 is slightly less good than N_1. Furthermore, the peak of S_{yp} of the closed loop (M-N) is $9.05dB$ corresponding to an unsatisfactory robustness margin. Conversely, reduced feedback controller K_3 provides better robustness margin for the closed loop (G-K) in comparison with the nominal one.

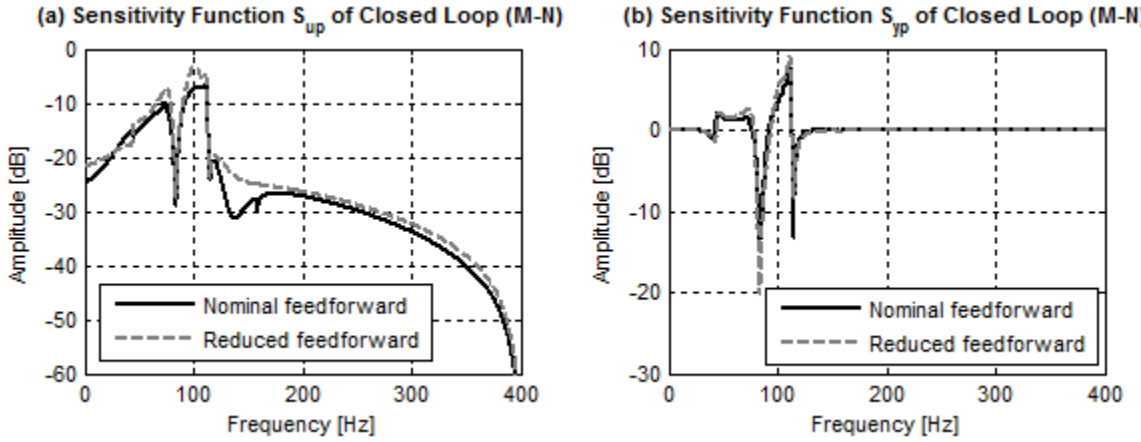

Figure 32. Sensitivity functions comparison for the feedforward controller

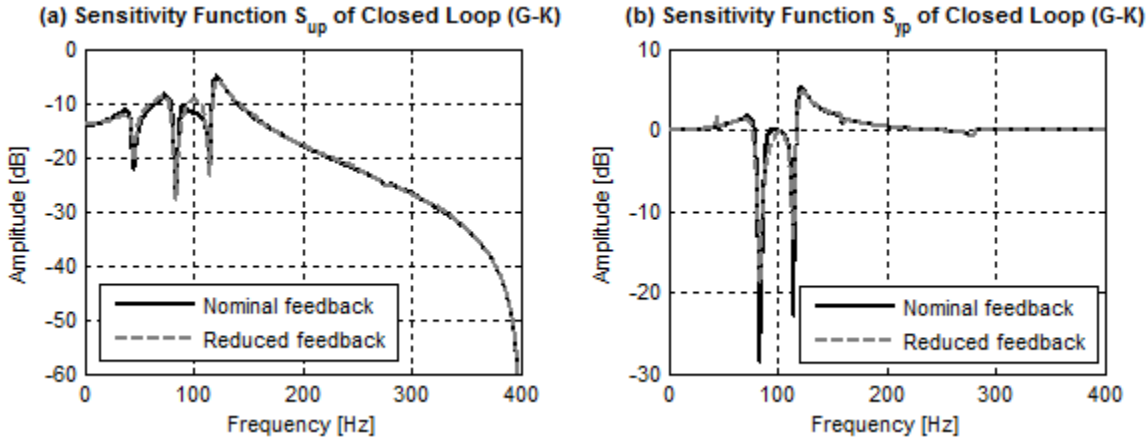

Figure 33. Sensitivity functions comparison for the feedback controller

Appendix C
Re-design and tuning of central controllers

This section extends the result of the Section 2 by taking into account the presence of broadband and narrowband disturbances. The objective is to maintain the level of performance as the system behavior with central controllers under the presence of broadband disturbances. The approach here is to re-design the compensators.

The objective is to design two filters $N(q^{-1})$ and $K(q^{-1})$ such that the effect of the disturbance $s(t)$ (including broadband and a sinusoidal disturbance at $150Hz$) on the output $v(t)$ be attenuated.

The formulation is the same as in Section 3. The selection of weighting functions is similar with the selection in Sections 4 and 5. The resulting controllers are the same as the case of re-design only feedback central compensator. The resulting feedforward compensator has almost no gain at $150Hz$ (not be presented here). The resulting feedback compensator inputs significant power at such frequency.

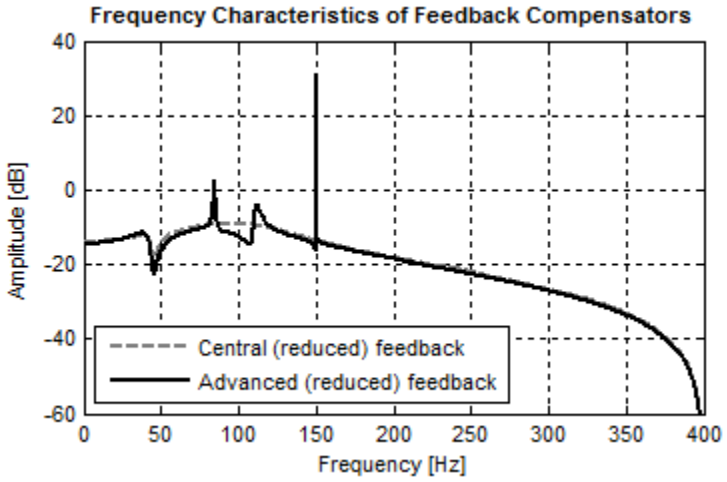

Figure 34. Frequency characteristics of nominal advanced feedforward & feedback compensators

In order to simplify the resulting controllers, it is needed to analyze the frequency characteristics of resulting compensators. From Fig. 34, one observes that the fixed part of the feedback controller denominator $H_{S_K}(q^{-1})$ has a pair of undamped complex zeros at $150Hz$. Hence, it can be factorized as

$$H_{S_K}(q^{-1}) = S_{BSF}(q^{-1})H^1_{S_K}(q^{-1})$$

where $H^1_{S_K}(q^{-1})$ associates to other control specifications (in this case, it is equal to 1).

Hence, we will look for reduced order feedback controllers with the fixed parts: $H_{S_K} = S_{BSF}$, $H_{R_K} = 1 + q^{-1}$. For feedforward controller, the fixed parts have been chosen as same as in Appendix B. Good results were obtained with reduced feedforward filter of order $n_{B_{\tilde{N}}} = n_{A_{\tilde{N}}} =$

5, $n_{\hat{N}} = 0$ and reduced feedback filter of order $n_{B_{\hat{K}}} = n_{A_{\hat{K}}} = 17$, $n_{\hat{K}} = 0$. The reduced order feedforward compensator obtained is similar with central one and will not be presented here. The reduced order feedback compensator obtained is shown and be compared with the central one in Fig. 35.

The performance of the system is illustrated by experimental results in Fig. 36. The disturbance includes PRBS and a sinusoidal disturbance of $150Hz$ with the magnitude are 0.1 and 0.3, respectively. One can observe that the advanced compensators introduces a strong attenuation of the sinusoidal disturbance (about $30dB$) without affecting other frequencies.

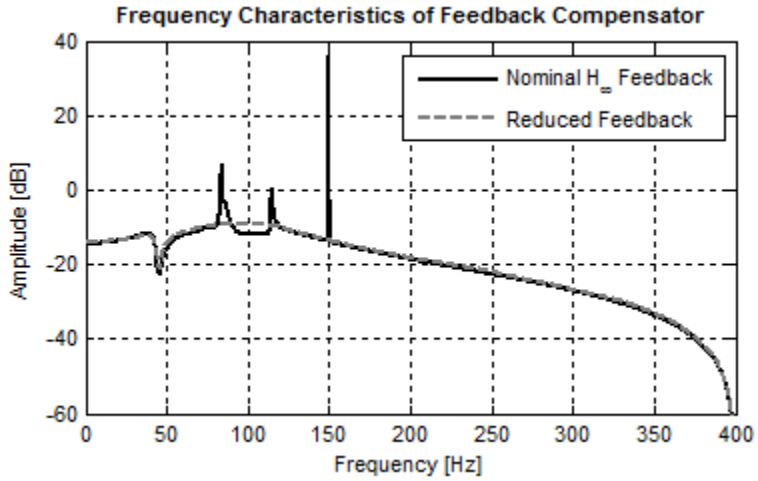

Figure 35. Frequency characteristics of (reduced) advanced and central feedback compensators

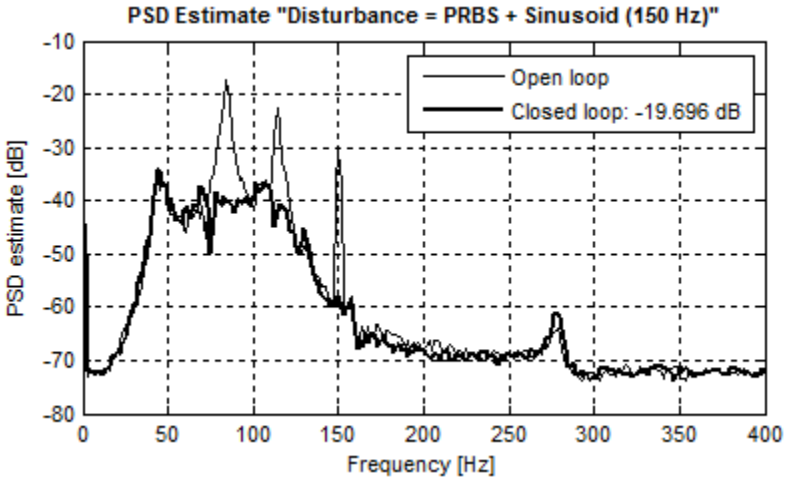

Figure 36. Power spectral densities of the residual acceleration (Disturbance = PRBS + Sinusoid 150Hz)

As can be seen from Fig. 37, similar results are obtained with multiple narrowband disturbances (with nominal compensators, not reduced-order compensators). An important remark is that attenuation of broadband and two sinusoidal disturbances is a level large enough in most applications.

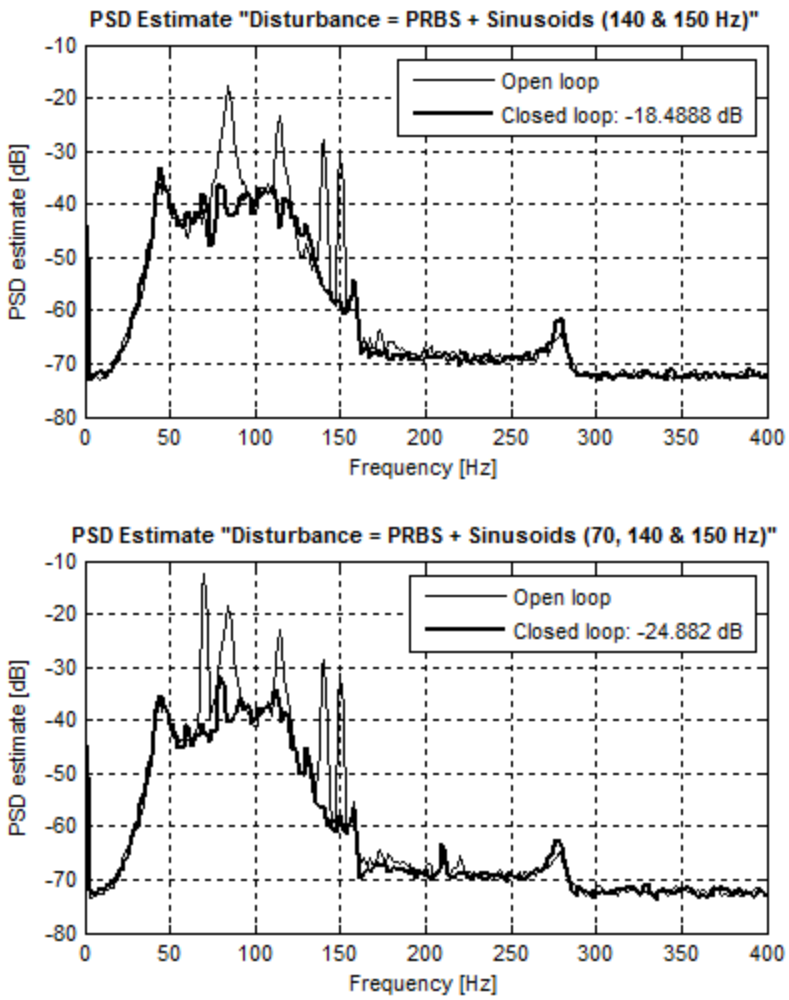

Figure 37. Power spectral densities of the residual acceleration (Disturbance = PRBS + Multi-Sinusoids)

The re-computing of only feedback controller (or only feedforward controller) has been obtained using the same procedure by considering new plant including the original plant and central feedforward (or feedback) compensator. The resulting controllers and performances are similar as in Sections 4 and 5, thus, will not be presented here.

References

1. Landau ID, Zito G, *Digital Control Systems*, Springer London 2005.
2. Zhou K, Doyle JC, *Essentials of Robust Control*, NY: Prentice-Hall 1998.
3. Alma M, Martinez JJ, Landau ID, Buche G. Design and tuning of reduced order h-infinity feedforward compensators for active vibration control, *Control Systems Technology, IEEE Transactions on* 2011.
4. Landau ID, Karimi A, Constantinescu A. Direct controller order reduction by identification in closed loop, *Automatica* 2011.
5. PhD theses of Alma M (2009), Airimitoaie TB (2012)
6. Landau ID, Castellanos Silva A, Airimitoaie TB, Buche G, Noe M. Benchmark on adaptive regulation – rejection of multiple unknown/time-varying narrow band disturbances, *European Journal of Control* 2013.